

Review of recent results on spin polarized tunneling and magnetic switching by spin injection

A. Fert^a, A. Barthélémy^a, J. Ben Youssef^c, J.-P. Contour^a, V. Cros^a,
J.M. De Teresa^a, A. Hamzic^a, J.M. George^a, G. Faini^{b,*}, J. Grollier^a, H. Jaffrès^a,
H. Le Gall^c, F. Montaigne^a, F. Pailloux^a, F. Petroff^a

^a *Unité Mixte de Physique CNRS-Thomson CSF, 91404 Orsay, France*

^b *L2M-CNRS, 92250 Bagneux, France*

^c *Laboratoire de Magnétisme de Bretagne, 29285 Brest, France*

Abstract

We review recent results obtained at Orsay on two topics in the field of spin electronics: (i) Spin polarized tunneling in magnetic tunnel junctions combining electrodes of ferromagnetic transition metal and half-metallic oxide: we will describe the influence of the nature of the barrier on the sign of the spin polarization of electrons tunneling from the transition metal and we also discuss the temperature dependence of the TMR obtained with half metallic oxides. (ii) Magnetization reversal by spin injection: we will present and interpret experimental results obtained with pillar-shaped Co/Cu/Co trilayers. © 2001 Elsevier Science B.V. All rights reserved.

Keywords: Spin polarized tunneling; Magnetic switching; Spin injection

1. Introduction

We present a review of recent results obtained at Orsay on two topics in the field of spin electronics: (i) spin polarized tunneling in magnetic tunnel junctions, and (ii) magnetization reversal by spin injection. The first topic is presently a very active field of research and the magnetoresistance (TMR) of magnetic tunnel [1,2] is promising for important applications (in particular for Magnetic Random Access Memories or MRAM, see article of S.S.P. Parkin in the same issue [3]). Although some applications of TMR are already in development, the physics governing the spin polarization of tunneling electrons is still far from being well understood. For example, whereas the polarization of the probability of tunneling from a ferromagnetic metal is expected to be the polarization of the density of states (DOS) at the Fermi level, the positive polarization found for electrons tunneling from most ferromag-

netic transition metals through alumina [4] disagrees with the negative polarization of their DOS. We have studied junctions in which the same electrodes are separated by different barriers. Our experimental results show that the sign and amplitude of the polarization depend on the nature of the tunnel barrier and we will discuss the role of the electronic bonding at the electrode/barrier interface in determining this polarization. The results we present are obtained in junctions in which one of the electrodes is made of a half-metallic oxide and we also emphasize the interest of half-metals in the race to very high TMR.

The second part of the paper is devoted to magnetic switching by spin injection. The mechanism by which a magnetic moment can be reversed by injecting a spin polarized current has been introduced by Slonczewski [5] and the existence of such effects has been recently confirmed by experiments [6–9]. We will present experimental results we have obtained on Co/Cu/Co trilayered pillars in which the current polarized by a thick Co layer is used to reverse the magnetization of a thinner second Co layer.

* Corresponding author. Tel.: +33-1-42317430; fax: +33-1-42317378.

2. Spin polarized tunneling in magnetic tunnel junctions

We present experimental results on magnetic tunnel junctions in which the bottom electrode is made of $\text{La}_{0.7}\text{Sr}_{0.3}\text{MnO}_3$ (LSMO) and the top electrode made of a ferromagnetic transition metal or alloy (Co, Fe or NiFe). We compare the TMR we obtain by using several types of barrier: SrTiO_3 (STO), $\text{Ce}_{1-x}\text{La}_x\text{O}_y$ (CLO), Al_2O_3 (ALO) and also an hybrid barrier (ALO/STO). We have grown (laser ablation, epitaxial growth) LSMO on a STO (100) substrate and STO or CLO on top of LSMO. ALO is obtained by sputter deposition of Al and plasma oxidation. The transition metal is deposited by sputtering or MBE. Details on the fabrication have been given elsewhere [10,11]. Lithographic patterning is used to fabricate junctions with sizes ranging between $10 \times 10 \mu\text{m}^2$ and $50 \times 50 \mu\text{m}^2$.

We recall that LSMO is a half-metallic oxide with a very high spin polarization. TMR experiments [12–16] on LSMO/STO/LSMO junctions have found polarizations between 70% and 85%. The positive sign of this polarization, expected from the double exchange model, has been clearly confirmed by the measurements of Worledge et al. [17] on LSMO/STO/Al junctions (+72%), positive polarization meaning higher tunneling probability for the majority of spin electrons. In our experiments we use a half-metallic LSMO electrode as an analyzer of the spin polarization of the electrons tunneling from a transition metal. A positive polarization of the transition metal (like that of LSMO) is expected to give a normal TMR, that is a higher resistance in the antiparallel (AP) magnetic configuration of the electrodes. On the contrary, a negative polarization should give an inverse TMR, that is a higher resistance in the parallel (P) state. This can be shown from general arguments or also, for example, from a Jullière-like expression of the TMR, $(R_{\text{AP}} - R_{\text{P}})/R_{\text{P}} = 2 P(\text{LSMO}) P(\text{Co})/[1 + P(\text{LSMO}) P(\text{Co})]$, where $P(\text{LSMO})$ and $P(\text{Co})$ are the respective spin polarization of the tunneling probability from LSMO and Co.

In Fig. 1, we compare TMR curves recorded at low bias for six types of junction: Fe/STO/LSMO in (a), $\text{Ni}_{40}\text{Fe}_{60}$ /STO/LSMO in (b), Co/STO/LSMO in (c), Co/CLO/LSMO in (d), Co/ALO/LSMO in (e) and Co/ALO/STO/LSMO in (f). Some of these results have already been reported in Ref. [10,18].

The normal TMR seen in (e) for Co/ALO/LSMO confirms the positive polarization of the tunneling probability from Co when the barrier is ALO [4]. In contrast, with the same Co and LSMO electrodes but when the ALO barrier is replaced by STO in (c) or CLO in (d), the TMR is inverse. This means that the polarization of cobalt is negative when the tunneling is through STO or CLO (same sign as for the polarization of the density of states of the d band of Co at the Fermi level). The TMR of Fe/STO/LSMO in (a) and

$\text{Ni}_{40}\text{Fe}_{60}$ /STO/LSMO in (b) are also inverse, which indicates that, with STO, the polarizations of Fe and $\text{Ni}_{40}\text{Fe}_{60}$ are also negative. Other recent experiments [19] have also seen an influence of the barrier on the polarization of tunneling (negative polarization of permalloy with Ta_2O_5).

The above results on the role of the nature of the barrier in determining the sign of the spin polarization is consistent with several recent ab initio calculations. According to the calculations of Nguyen Manh et al. [20], de Boer et al. [21], Oleinik et al [22] or Tsymbal et al. [23], the polarization of tunneling electrons is governed by the mechanism of electronic bonding at the metal/oxide interface (covalent bonding between Co and O at the interface of Co with O terminated ALO or hybridization between Co and Al at the interface of Co with Al terminated ALO). Our results confirm that, for the same Co electrode, different types of barrier and thus different types of bonding can produce different amplitudes and different signs of the polarization. That the influence of the barrier on the sign of the polarization is mainly due to interface effects is confirmed by the results of Fig. 1f for a Co/ALO/STO/LSMO junction. Although the thicker part of the barrier is made of STO, the TMR is normal which suggests that the existence of a Co/ALO interface is more important than the global composition of the barrier. So far ab initio calculations have been published only for interfaces of ferromagnetic metals with ALO, HfO_2 and ZnSe [20–24]. The same type of calculation for interfaces of transition metal with STO would be also of great interest [25].

Different types of barrier produce not only different signs of spin polarization but also very different bias dependence of the TMR. Several examples of bias dependence are shown in Fig. 2. For Co/ALO/STO/LSMO, we observe the classical rapid decrease of the TMR as a junction of the bias which is generally found in junctions with ALO. For the three junction with STO in Fig. 2, the bias dependence is different from that with ALO, with a definite asymmetry between positive and negative bias and a marked maximum of TMR at negative bias (negative meaning electrons going from LSMO to TM). However there are also definite differences between junctions with Co, Fe and $\text{Ni}_{40}\text{Fe}_{60}$. For the junctions with Co, we find a maximum of TMR at a relatively higher voltage (-0.4 V) than for Fe and $\text{Ni}_{40}\text{Fe}_{60}$. For Co and NiFe but not for Fe, the sign of the TMR changes above about $+0.7$ V (crossover to normal TMR). In contrast, Fe/STO/LSMO exhibits a characteristic second peak in positive voltage. It thus turns out that, with STO, each transition metal has a specific signature in the bias dependence, probably related to the specific profile of the density of states of its d band.

The behavior described above, that is mainly inverse TMR and typical bias dependence, has been now observed in TM/STO/LSMO junctions prepared by various methods [26]. We want also to point out that, in our experiments, we find this behavior in a broad range of barrier thickness and junction size, that is for junction resistances ranging from about 200Ω (Fig. 1c) to almost $10^8 \Omega$ (Fig. 1a). In particular this rules out any influence of geometrical effects [27] or metallic contacts

through pinholes the barrier [28] that could be suspected for junctions with only low resistance.

All the results we described so far have been obtained at low temperature. An important issue for LSMO-based junctions is also the temperature dependence of the TMR. In junctions of the type LSMO/STO/LSMO, it has been generally found [12–16] that the TMR decreases rapidly with temperature and vanishes at a relatively low temperature T_{CI} . In previous experiments

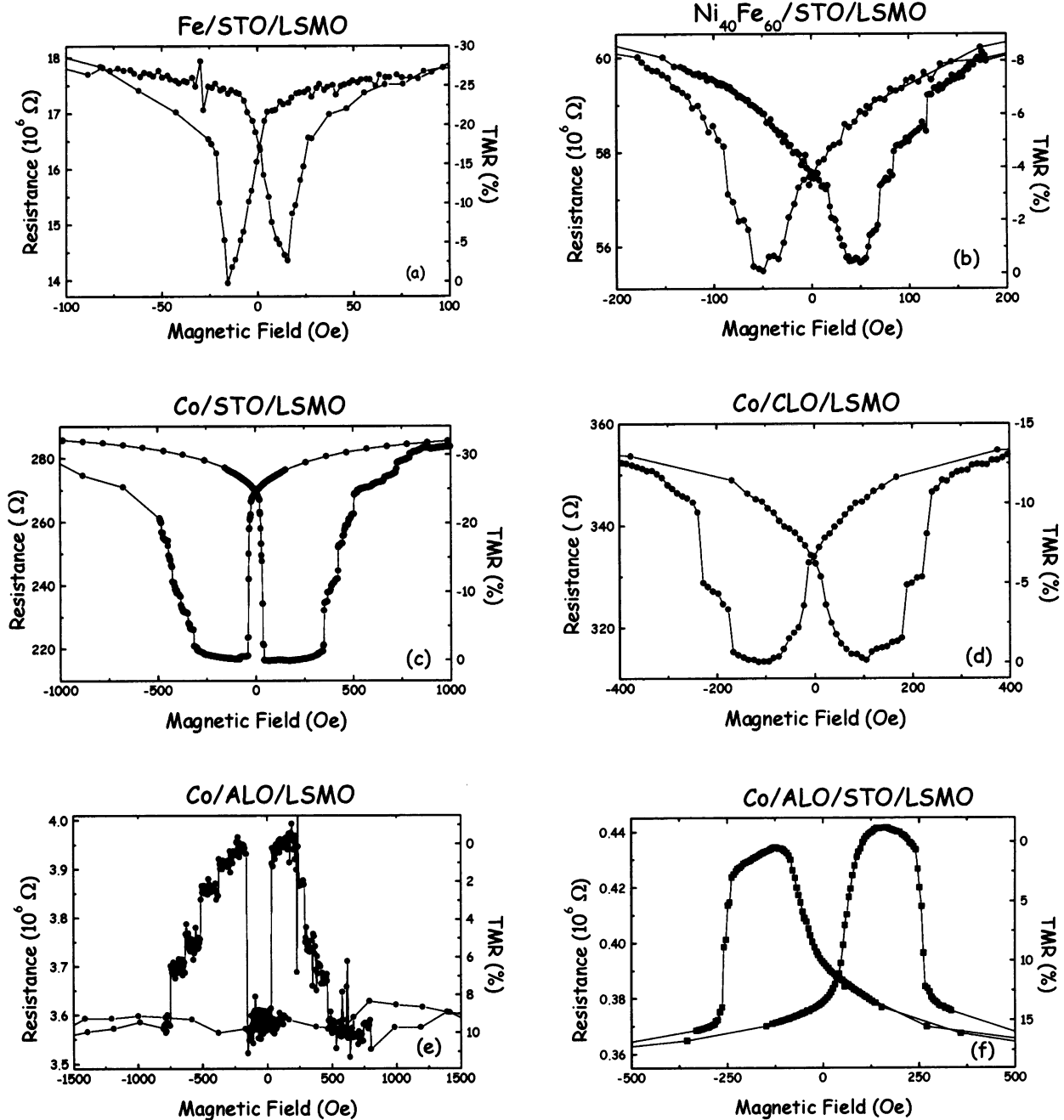


Fig. 1. TMR curves of six TM/I/LSMO tunnel junctions at 40 or 50 K for: (a) Fe/STO/LSMO, (b) $Ni_{40}Fe_{60}$ /STO/LSMO, (c) Co/STO/LSMO, (d) Co/CLO/LSMO, (e) Co/ALO/LSMO, and (f) Co/ALO/STO/LSMO. The curves are recorded at -0.01 V, except for (a) (-0.1 V) and (b) (-0.4 V). The barrier thickness is 3 nm for STO in (a) and (b), 2 nm for STO in (c), 2.5 nm for CLO in (d), 3 nm for ALO in (e), 1.5 nm for ALO and 1 nm for STO in (f).

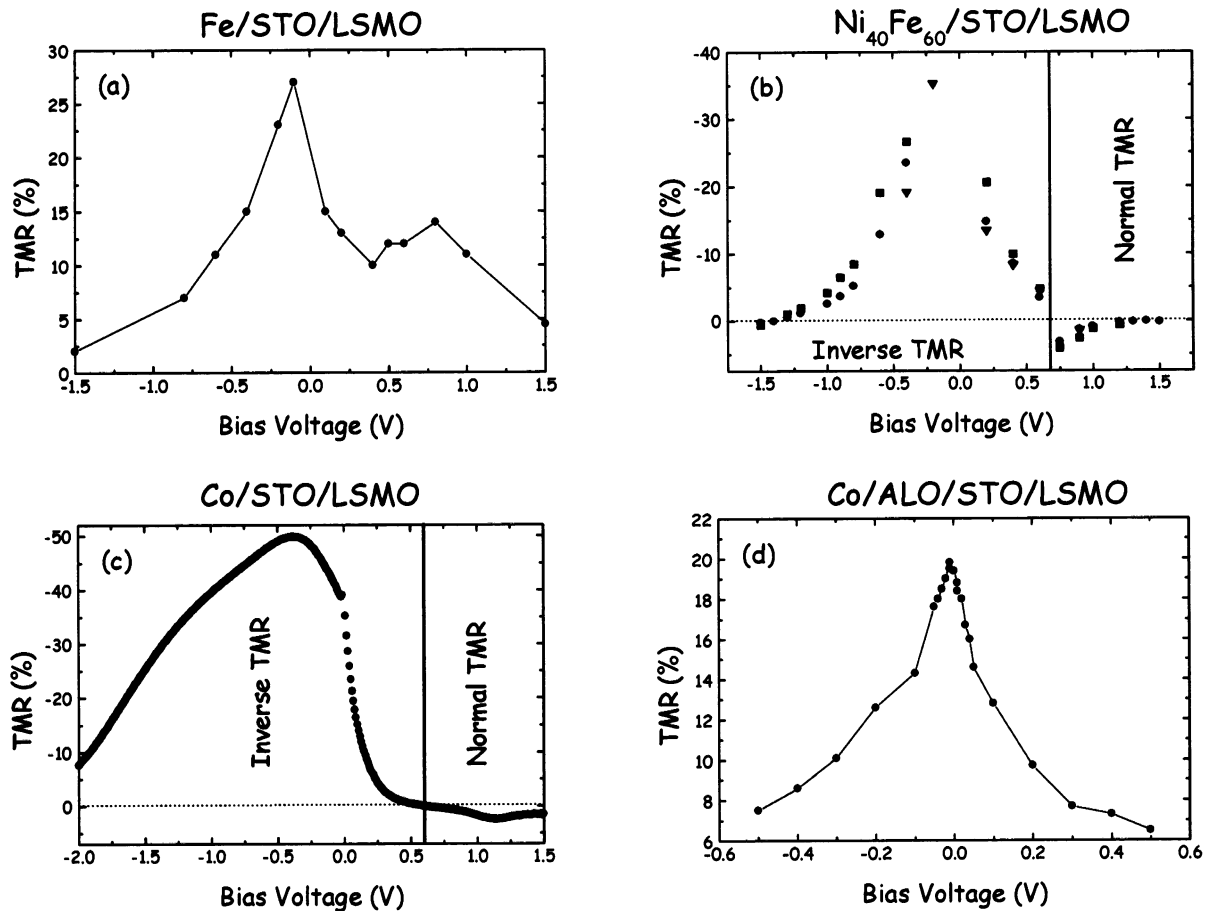


Fig. 2. Bias dependence of the TMR at 40 K for Fe/STO/LSMO, $\text{Ni}_{40}\text{Fe}_{60}$ /STO/LSMO, Co/STO/LSMO and Co/ALO/STO/LSMO tunnel junctions. Note the different scale for Co/ALO/STO/LSMO.

in our group, T_{CI} is typically around 200K, well below the Curie temperature of LSMO, $T_c \approx 340\text{--}370$ K. We ascribed this collapse of TMR at about 200 K to a reduction of the Curie temperature by disorder at the interface with the barrier, so that the TMR vanishes at the interface Curie temperature, $T_{\text{CI}} \cong 200$ K. This reduction of the Curie temperature in an interfacial layer is also indicated by the maximum of tunnel resistance observed at about 200 K (we recall that, in LSMO, the number of carriers progressively decreases as T increases from the low temperature limit to the metal–insulator transition at the Curie temperature, what gives rise to a maximum of resistance and tunnel resistance at this temperature). However, in the junctions TM/STO/LSMO described in the present article, the temperature dependence is less dramatic. For the Sample 1 in Fig. 3a, the TMR disappears at a temperature very close to the Curie temperature of bulk LSMO and still amounts at 5% at 300 K. Accordingly we see in the inset of Fig. 3b that the maximum of tunnel resistance, associated with the Curie temperature at the interface, is also above 300 K. This means that the rapid drop of the interface polarization with temperature previously observed in LSMO/STO/LSMO junctions is not intrinsic

for LSMO interfaces and, in junctions prepared in the same conditions but with two LSMO electrodes, should probably be ascribed to their top LSMO/STO interface. This could be due, for example to a more disordered structure for the top interface or also, possibly, to different termination of LSMO and STO at the bottom and top interfaces.

We also emphasize that the temperature dependence of the tunnel resistance provides us with an interesting tool to probe the ‘quality’ of the LSMO/barrier interfaces. In Fig. 3 we also show our results for the Sample 2 which, in contrast with Sample 1, exhibits a maximum of tunnel resistance below room temperature. It can be seen that, accordingly, there is no TMR at room temperature. The lower ‘quality’ of the LSMO/STO interface in Sample 2 also appears in the negative slope of the high field TMR (Fig. 3c) which reflects the field induced re-ordering of a magnetically disordered interface. In contrast the absence of high field TMR in Fig. 3a for Sample 1 confirms the magnetic quality of the LSMO/STO interface of this sample.

That the TMR of junctions with manganites does not necessarily vanish well below the bulk Curie temperature is an interesting result in the perspective of RT

tunnel devices. It is clear that the manganites themselves, with T_C just above RT, cannot be used for applications of TMR at RT. However other families of half-metallic oxides having a definitely higher Curie temperature are now emerging [29] and can lead to very high TMR effects at RT.

3. Magnetization reversal by spin injection

In this section we present experimental results on magnetic switching by spin injection that we have obtained on pillar-shaped Co/Cu/Co trilayers. These experiments, as those of Katine et al. [9] on similar pillars, demonstrate the existence of the effects predicted by Slonczewski [5] in 1996 and also theoretically studied in several recent publications [30–33]. We will summarize our results and a detailed report will be presented elsewhere.

Our samples are obtained by a process including successively patterning of the bottom electrode and fabrication of a template for the pillar by e-beam lithography, sputter deposition of a Co/Cu/Co trilayer into the template, and finally deposition of a gold upper contact on the top of the pillar. The successive stages of the process are illustrated in Fig. 4. In the experimental results described below, the trilayers are composed of a thick Co layer (15 nm) and a thin Co layer (2.5 nm) separated by a Cu layer of 10 nm. The pillars have various shapes, from $100 \times 100 \text{ nm}^2$ to $200 \times 600 \text{ nm}^2$. A d.c. current is passed through the pillar to switch the magnetic configuration and also to detect the switching by GMR effect.

In Fig. 5 we present an example of CPP-GMR obtained with a small current of $50 \mu\text{A}$ and a magnetic field applied along the longer side of a rectangular pillars. The magnetoresistance is small ($\sim 0.5\%$), which is due to the relatively small contribution of the Co/Cu/Co trilayer to the total resistance of the pillar. However

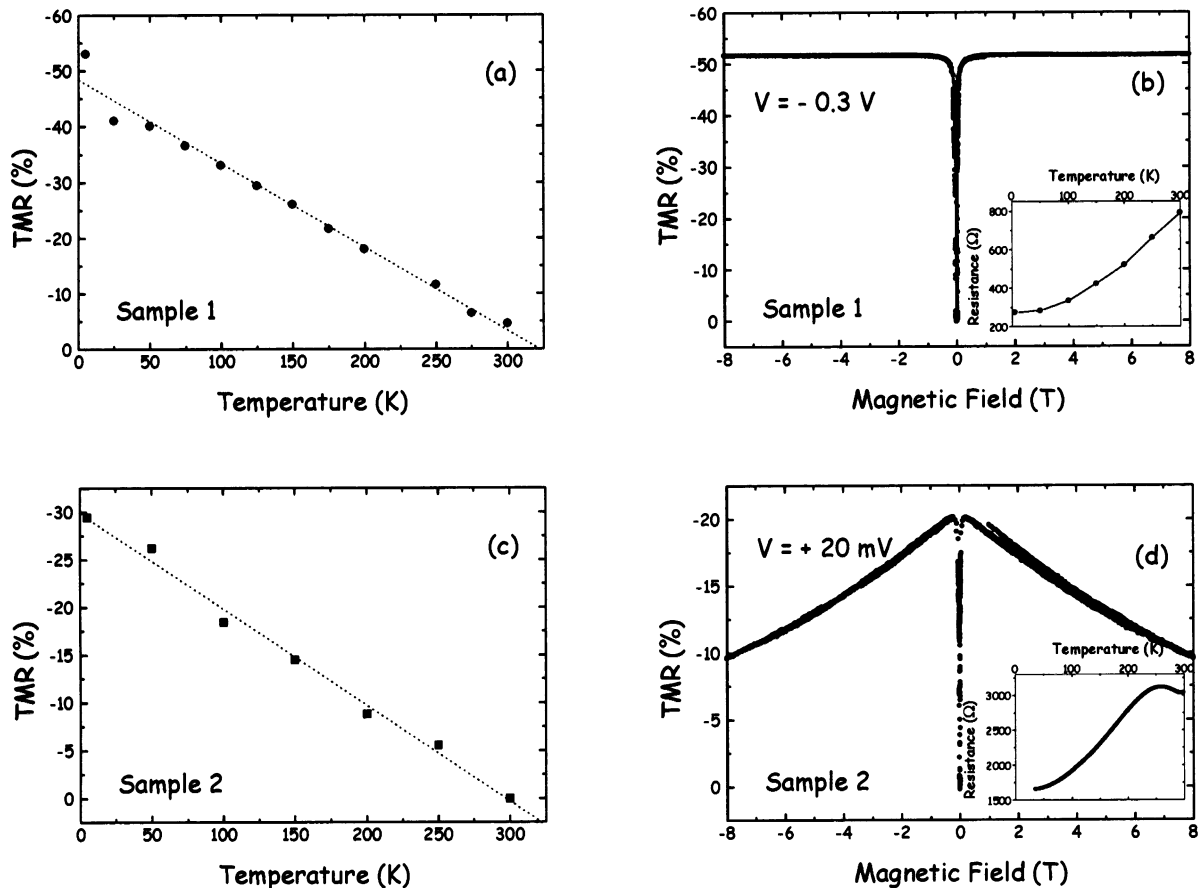


Fig. 3. Temperature dependence of TMR at -0.4 V (voltage giving the maximum value of TMR), high field MR at 5 K and, in the insets, tunnel resistance R_T (in Ohm) versus temperature for two Co/STO/LSMO tunnel junctions, Sample 1 (top) and Sample 2 (bottom). The increase of R_T with T reflects the decrease of carrier density with spin disorder and its maximum, as for the bulk resistivity, indicates the metal/insulator transition at the Curie temperature. For Sample 1 ('better sample'), the temperature of the maximum of R_T (\sim interface Curie temperature) is above RT, and accordingly, TMR still exists at RT. The quality of the LSMO/STO interface in Sample 1 is also seen in the absence of high field MR. For Sample 2, the maximum of R_T is below RT, the TMR is zero at RT and the stronger interfacial disorder is reflected by the decrease of resistance at high field (magnetic re-ordering by the applied field).

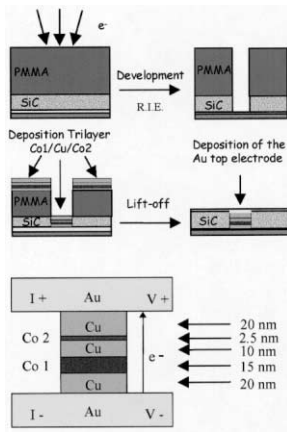


Fig. 4. Lithographic process for the fabrication of the Co/Cu/Co pillars and schematic of a pillar.

the typical features of GMR are clearly observed, with well defined field ranges of P (parallel) and AP (antiparallel, at least partly) configurations. To study the reversal of magnetization induced by an increase of the current, it is important to know precisely the initial configuration before the current is increased. In the experiments described below, we started from A (or A*) in zero field on the GMR curve in decreasing (increasing) field on Fig. 5, that is a P configuration with the magnetic moments of both Co layers in the direction of positive (negative fields).

In Fig. 6 we present the variation of the resistance R of the pillar when, starting from the P configuration at A in Fig. 5, we increase or decrease the current I (in our notation, positive I means electrons going from the thick Co layer to the thin one). For $I > 0$, nothing occurs except a gradual and reversible rise of R along a curve that we call $R_p(I)$. This gradual rise, as in the data reported by Katine [9], can be attributed to some enhancement of the scattering for hot electrons. For

$I < 0$, the system first moves reversibly on $R_p(I)$ and then jumps into a high resistance state at $I_c^P \cong -15$ mA. After the jump, when I varies between its maximum negative value and $I_c^{AP} \cong +15$ mA, the system moves on a high resistance curve that we call $R_{AP}(I)$. When I exceeds $I_c^{AP} \cong +15$ mA, the resistance drops on the $R_p(I)$ curve. The difference of about 1 m Ω between $R_{AP}(I)$ and $R_p(I)$ corresponds approximately to the amplitude of the GMR in Fig. 5, which indicates that the system is switched from P to AP at I_c^P and from AP to p at I_c^{AP} .

The curves of Fig. 6 were recorded in zero field. In applied field, I_c^P increases and I_c^{AP} decreases, as expected from a stabilization of the parallel configuration by an applied field. At high enough field (above 5 kOe), the trilayer is still pinned in the P configuration at our highest current value and the background curve $R_p(I)$ can be recorded throughout the whole experimental range of I .

The results described above are in agreement with the predictions of Slonczewski [5] and the previous results of Katine et al. [9] on pillars (we point out the opposite conventions for the sign of I in Katine et al. and the present paper). An essential feature of these results is that the switching from P to AP and from AP to P are respectively induced by negative and positive currents. This definitely distinguishes the magnetization reversal by spin injection from the possible reversal by the magnetic field generated by the current. A reliable test is the comparison of the $R(I)$ curves recorded after starting respectively from the points A (parallel magnetizations in the positive direction) and A* (magnetizations in the negative direction). If the switching of the configuration A was due to the field generated by a negative current, the configuration A* should be switched by the field generated by a positive current. On the contrary, we find that the $R(I)$ curves are the

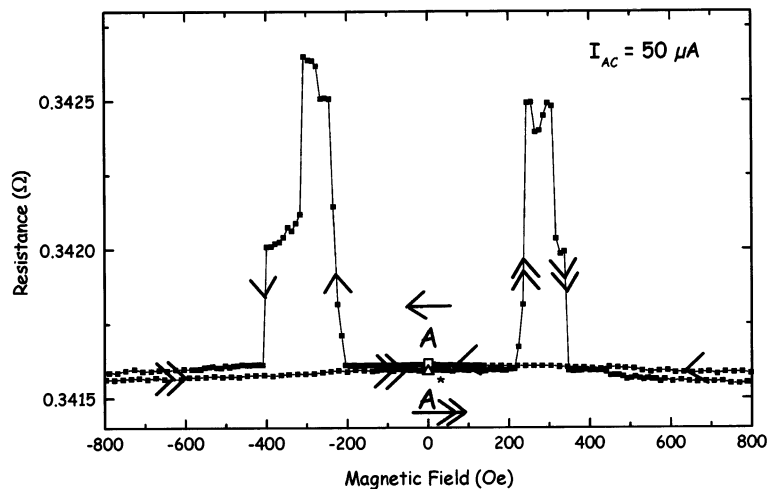


Fig. 5. GMR curve of a 200×600 nm² Co/Cu/Co pillar (Sample 1) at 4.2 K with $I_{AC} = 50$ μ A. A and A', at zero field on the curves in decreasing and increasing field respectively, are the starting point of the experiments in Fig. 6.

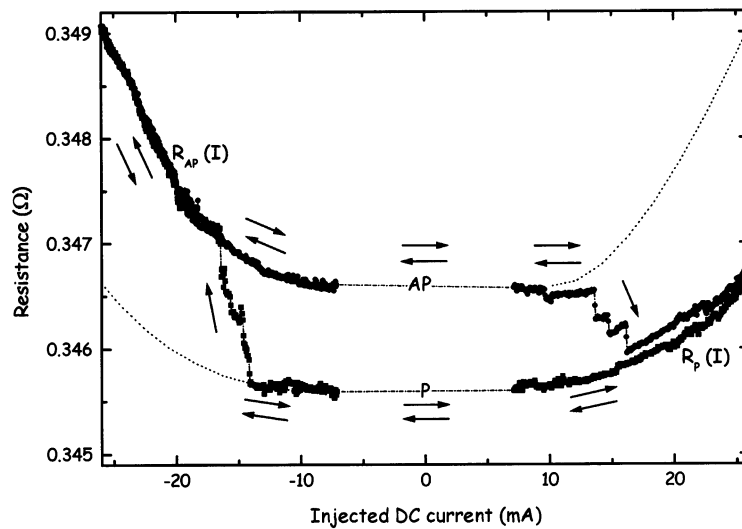


Fig. 6. Resistance as a function of DC current for the sample of Fig. 5. Single arrows (double arrows) indicate the irreversible (reversible) parts of the cycle. The measurements at low current (flat part of the variation) were noisy for technical reasons and have not been put on the figure. The dotted lines have been obtained by symmetry and are guides for the extrapolation of $R_{AP}(I)$ and $R_P(I)$.

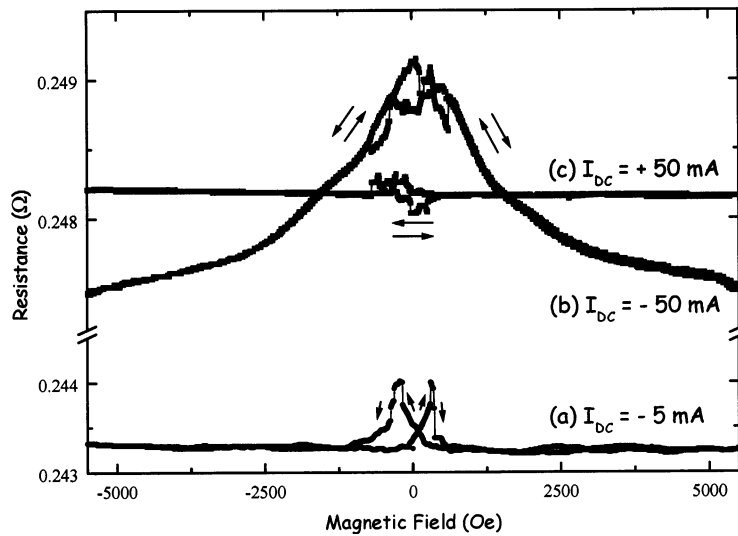


Fig. 7. Resistance as a function of the applied field for a $(200 \times 600) \text{ nm}^2$ pillar (Sample 2). The current is: -5 mA for curve (a), -50 mA for (b) and $+50 \text{ mA}$ for (c).

same in both cases, which is expected only from spin injection effects. In other words, an essential feature of the reversal by spin injections is that, whatever the initial orientation of the magnetizations, the cycle of Fig. 6 can only be clockwise. The only departure from theory is that we find approximately equal values of I_c^{AP} and I_c^P in zero applied field, whereas the model of Slonczewski [5] predicts a marked asymmetry between these two critical currents. This will be discussed later.

In Fig. 7 we present a second type of experimental approach in which we sweep the magnetic field between -5.5 kOe and $+5.5 \text{ kOe}$ at constant current. In a small current ($5 \mu\text{A}$), we observe typical curves of

GMR in uncoupled trilayers, with split sharp MR peaks in increasing and decreasing field which reflect a partial AP ordering in the field range between the coercive fields of the two layers. For $I = -50 \text{ mA}$, the split peaks are replaced by a reversible broad peak extending from approx. -2500 Oe to $+2500 \text{ Oe}$, so that the MR curve looks like the GMR curve of a trilayer with strong antiferromagnetic coupling. The height of the broad peak also suggests that one reaches a higher degree of AP configuration than in the sharp peaks observed at small current. In contrast, with $I = +50 \text{ mA}$, the GMR effect disappears and $R(I)$ is a horizontal flat line, as what is expected for a ferromagnetic coupling.

The behavior in Fig. 7 confirms that a negative current induces an AP configuration, whereas a positive current pins the system in a P configuration. Does this mean that the effect of the current can be described by an effective interaction between the magnetic moments of the two layers, like the NEXI interaction introduced by Heide et al. [33]? As a matter of fact, the results of Fig. 7 are consistent with both the NEXI picture and Slonczewski's model. For example, the curve in Fig. 7 with $I = -50$ mA can be described in the model of Slonczewski as follows: starting from a parallel configuration at $H = +5.5$ kOe and decreasing the field, the negative current reverses the magnetization of the thin Co layer when the field is small enough and the configuration becomes AP, in agreement with the resistance rise in the peak; then, in turn, the magnetization of the thick layer is reversed when the applied field becomes negative but, since the resulting P configuration is unstable in a negative current, the magnetization of the thin layer is also reversed and the system practically remains in its AP configuration; finally a sufficient negative field induces again a P configuration and the resistance drops back to its initial value. We conclude that, at the present stage, our experimental results, do not allow us to decide between the Slonczewski and NEXI pictures.

We have based the quantitative interpretation of our experiments on a model combining Slonczewski's equations of motion [5] with a calculation of the current polarization from the equations developed in the VF model of the CPP-GMR [34]. Details on the calculation will be reported elsewhere and here we present only the final expressions — similar to those of Katine et al. [9] — for the critical currents I_c^P and I_c^{AP} (we recall that, with our definition, I is positive when the electrons go from the thick to the thin layer):

$$I_c^{AP}(I_c^P) = +(-)\{eMA[2\pi M + (-)H]at\}/hP_1^{P(AP)} \quad (1)$$

where M is the magnetization, H the magnetic field (applied + dipolar), t the thickness of the thin layer, P_1^P (P_1^{AP}) the current spin polarization calculated in the VF model for the P (AP) configuration, α is the Gilbert coefficient and A is the area of the pillar.

With the values of the resistivities, interfaces resistance, spin asymmetry coefficients β and γ and spin diffusion length in Cu derived by Bass and Pratt [36] for Co/Cu multilayers and the spin diffusion length in Co found by Fert and Piraux [35], we obtain $P_1^P = 0.26$ and $P_1^{AP} = 0.075$. By introducing these polarization in Eq. (1) with $M = 1420$ emu cm⁻³, and $\alpha = 0.007$ [37] we obtain for $H = 0$:

$$I_c^P = -15 \text{ mA (current density} = 1.25 \times 10^7 \text{ A cm}^{-2}\text{)}$$

$$I_c^{AP} = +55 \text{ mA (current density} \cong 4.5 \times 10^7 \text{ A cm}^{-2}\text{)}.$$

As the critical current in our experiments are around 15 mA (1.25 A cm⁻²), we see that the Slonczewski model predicts very correctly the order of magnitude for the critical current. On the other hand, the calculation predicts an asymmetry between the absolute value of the critical currents that we do not find in our experiments. Let us summarize the calculated and experimental data on this asymmetry: the initial model of Slonczewski predicts $g(\pi) > g(0)$ and thus $|I_c^P| > |I_c^{AP}|$, the present calculation using a GMR model to introduce the current polarization in Slonczewski model finds $|I_c^P| < |I_c^{AP}|$; which is in agreement with the experimental curves presented by Albert et al. [9] but not with our finding, $|I_c^P| \cong |I_c^{AP}|$. Another problem is the field dependence of the calculated critical currents which is less pronounced than in our experimental results. For $|I_c^P|$, for example, the fit with our experiment results would require an enhancement of the Gilbert coefficient by a factor of about 5.

Recently one of us (AF) has also participated to the development of another type of model based on the calculation of the spin accumulation energy generated by spin injection. This model will be published elsewhere [38]. The effect of the current is described by an effective interlayer coupling. The prediction for the order of magnitude of the critical current of switching is also in agreement with our experiments.

4. Conclusion

We summarize the main results discussed in the paper:

In tunnel junctions of the type TM/I/LSMO [10,18], where TM is a transition metal (Co, Fe or NiFe), we find that the sign of the spin polarization of the tunneling probability from TM is different for different types of barrier I (example: $P(\text{TM}) > 0$ for $I = \text{ALO}$ and $P(\text{TM}) < 0$ for $I = \text{STO}$). This is in agreement with recent theoretical developments [20–23] which have shown that the spin polarization of tunneling electrons is governed by the specific type of electronic bonding at the electrode/barrier interface.

There is still a TMR of 5% at 300 K in, for example, Co/STO/LSMO tunnel junctions. This means that, in junctions with half-metallic manganites, the TMR does not necessarily vanish at a temperature well below the Curie temperature ($T_c \cong 340\text{--}370$ K for LSMO). High TMR ratios at RT can probably be obtained with half-metallic oxides [29] having a higher Curie temperature than the manganites.

Our experimental results on magnetic switching by spin injection in pillar-shaped Co/Cu/Co trilayers, in agreement with previous results by Katine et al. [9], confirm the theoretical predictions of current driven interlayer coupling. In addition to measurements of

Katine's type, we have presented a new type of experiment (Fig. 7) which also evidences clearly the control of the magnetic configuration of the trilayer by the current intensity. We have also described an interpretation of our results mixing Slonczewski's equations with a calculation of the current spin polarization based on the VF model of CPP-GMR [34].

References

- [1] R. Jullière, Phys. Lett. A 54 (1975) 225.
- [2] J.S. Moodera, L.R. Kinder, T.M. Wong, R. Meservey, Phys. Rev. Lett. 74 (1995) 3273.
- [3] S.S.P. Parkin, in press.
- [4] R. Meservey, P.M. Tedrow, Phys. Reports 238 (1994) 173.
- [5] J. Slonczewski, J. Magn. Magn. Mat. 159 (1996) 1.
- [6] M. Tsoi, et al., Phys. Rev. Lett. 80 (1998) 4281.
- [7] E.B. Myers, et al., Science 285, 867
- [8] J.E. Wegrove, et al., Europhysics Lett. 45 (1999) 626.
- [9] A. Katine, et al., Phys. Rev. Lett. 84 (2000) 3149; F.J. Albert, J.A. Katine, R.A. Burhman, D.C. Ralph, Appl. Phys. Lett. 77 (2000) 3809.
- [10] J.M. De Teresa, A. Barthélémy, A. Fert, J.P. Contour, R. Lyonnet, F. Montaigne, P. Seneor, A. Vaurès, Phys. Rev. Lett. 82 (1999) 4288.
- [11] J. Nassar, M. Hehn, A. Vaurès, F. Petroff, A. Fert, Appl. Phys. Lett. 73 (1998) 698.
- [12] J.Z. Sun, Appl. Phys. Lett. 69 (1996) 3266.
- [13] M. Viret, M. Drouet, J-P. Contour, C. Fermon, A. Fert, Europhys. Lett. 39 (1997) 5.
- [14] J. O'Donnel, A.E. Andrus, S. Oh, E.V. Colla, D.N. Eckstein, Appl. Phys. Lett. 76 (1994) 2000.
- [15] Moon-Ho Jo, M.D. Mathur, N.K. Todd, M.G. Blamire, Phys. Rev. B 61 (2000) 14905.
- [16] Y. Luo, A. Kaufler, K. Samwer, Appl. Phys. Lett. 77 (2000) 1508.
- [17] D.C. Worledge, T.H. Geballe, Appl. Phys. Lett. 76 (2000) 900.
- [18] J.M. De Teresa, A. Barthélémy, A. Fert, J-P. Contour, F. Montaigne, P. Seneor, Science 286 (1999) 507.
- [19] M. Sharma, S.X. Wang, J.H. Nickel, Phys. Rev. Lett. 82 (1999) 616.
- [20] D. Nguyen-Mahn, E.Y. Tsybal, D.G. Pettifor, C. Arcangeli, R. Tank, O.K. Andersen, A. Pasturel, Mat. Res. Soc. Symp. Proc. 492 (1998) 319.
- [21] P.K. de Boer, G.A. de Wijs, R.A. de Groot, Phys. Rev. 58 (1998) 15422.
- [22] I.I. Oleinik, E.Y. Tsybal, D.G. Pettifor, Phys. Rev. B 62 (2000) 3952.
- [23] E.Y. Tsybal, I.I. Oleinik, D.G. Pettifor, J. Appl. Phys. 87 (2000) 5230.
- [24] J.M. MacLaren, X.G. Zhang, W.H. Butler, Xindong Wang, Phys. Rev. B 59 (1999) 5470.
- [25] D. Stoeffler, private communication.
- [26] H. Asano, et al., private communication; K. Steenbeck, et al., private communication.
- [27] J.S. Moodera, et al., Appl. Phys. Lett. 69 (1996) 70.
- [28] N. Garcia, M. Munoz, Y-W. Zhao, Phys. Rev. Lett. 82 (1999) 2923.
- [29] K.I. Kobayashi, T. Kimura, H. Sawada, K. Terakura, Y. Tokura, Nature 395 (1998) 677.
- [30] J.L. Berger, Phys. Rev. B 54 (1996) 9353.
- [31] Y.B. Bazaliy, et al., Phys. Rev. B 57 (1998) 3213.
- [32] J.E. Wegrove, preprint.
- [33] Heide, et al., Condensed Matter/0005064.
- [34] T. Valet, A. Fert, Phys. Rev. B 48 (1993) 7099.
- [35] A. Fert, L. Piraux, J. Mag. Mag. Mat. 200 (1999) 338.
- [36] J. Bass, W.P. Pratt Jr., J. Mag. Mag. Mat. 200 (1999) 274; Q. Yang, et al., Phys. Rev. Lett. 72 (1994) 3274.
- [37] F. Schreiber, et al., Sol. State Comm. 93 (1995) 965.
- [38] P.M. Levy, C. Heide, A. Fert, S. Zhang, in preparation.